JOURNAL OF CATALYSIS 1, 443–457

Structure and Properties of Evaporated Metal Films

J. R. ANDERSON AND B. G. BAKER,* AND J. V. SANDERS

From the Chemistry Department, University of Melbourne, and the Division of Tribophysics, C.S.I.R.O., Melbourne, Australia

Metal films particularly of nickel and tungsten, deposited on glass have been studied by electron microscopy in transmission and by replication, and by the measurement of gas adsorption and electrical resistance. From the transmission electron micrographs crystal widths have been obtained and the presence of gaps between the crystals established for nickel films examined as deposited at 273°K. On sintering, the first stage is the removal of intercrystalline gaps while in later stages surface asperities are removed and crystal growth occurs. The effect of sintering on gas adsorption and electrical resistance has been studied. From the extinction contours on individual nickel crystals in the transmission electron micrographs the detailed crystal shape has been deduced. Films deposited when the substrate was at an elevated temperature showed an area for gas adsorption considerably below that for films which had been sintered at that temperature subsequent to deposition at 273°K.

INTRODUCTION

Since the pioneering work of Beeck, Smith, and Wheeler (*1*), evaporated metal films have frequently been used for studying the chemical properties of metal surfaces. However, insufficient attention has been given to the bulk and surface structure of the films which are used. Many previous electron microscopic studies of film structure have used films deposited on organic substrates under relatively poor vacuum conditions, e.g. Picard and Duffendack (*2*), Levinstein (*3*), Milner and Tatarinova (*4*). Such films may differ from those deposited on baked glass under better vacuum conditions.

Sachtler, Dorgelo, and van der Knaap (*5*) have examined replicas of films deposited on glass and a number of studies have been made of the thermal stability of such films using an estimate of the surface area as an index of the degree of sintering, e.g. Beeck *et al.* (*1*), Gundry and Tompkins (*6*).

In the present work the more powerful technique of transmission electron microscopy has been used to measure the grain size in films of a number of metals; this has been related to the adsorption area. For nickel and tungsten films the electrical resistance has also been measured and the sintering behavior followed by all three techniques. Some sintering data for these metals has already been reported by Anderson and Baker (*7*).

EXPERIMENTAL

The cyclindrical Pyrex vessel, onto the inside wall of which the film was deposited, was attached to the vacuum line by a water-cooled ground-glass joint, lubricated by Apiezon-L grease. Figure 1 shows this and the geometric arrangement of the evaporation filament with respect to the vessel. The standard size vessel was of internal diameter 45 mm and length 130 mm over the region of uniform diameter. In a few experiments a larger diameter of 75 mm was used and in both cases the wall thickness was about 1 mm.

The details of evaporation of nickel and tungsten films have already been described (*7*). Films of rhodium, platinum, palla-

* Present address: Division of Tribophysics, C.S.I.R.O., Melbourne.

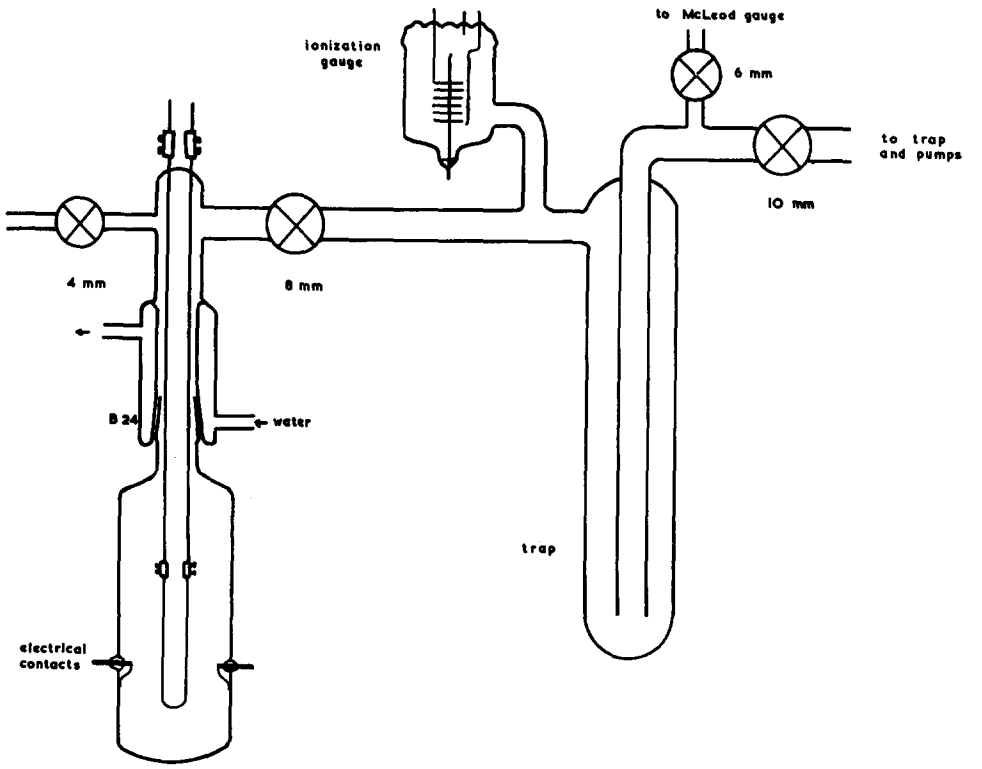

FIG. 1. Film deposition apparatus.

dium, molybdenum, and iron were prepared by essentially the methods described by Kemball (*8*) and Anderson and Kemball (*9*), except for the extension of the baking and outgassing periods to 15 hr.

Chromium films were evaporated from 0.5 mm diameter wire.* For the virgin wire the total metallic impurity was <30 parts/10^6, and the dissolved gas content was: O_2, 0.01% (W/W); S, 0.001%; N_2 0.0008%; H_2 0.0002%. Before use the chromium filament was purified by the evaporation of one film of about 10 mg weight and the subsequent evaporation was carried out at about 6 amp after outgassing for 2 hr at 4.6 amp.

In all cases the pressure in the evaporation vessel at the end of the baking and filament outgassing was about 2×10^{-7} mm Hg as measured by the ionization gauge attached at the head of the vessel. The pressure was measured during the evaporation of nickel and tungsten and no change was observed from the above value.

Surface areas of the films were measured by the BET method using the adsorption of xenon at 90°K as described by Anderson and Baker (*7*).

Resistance measurements were made on films deposited in a vessel of standard dimensions, contact with the film being made with pieces of platinum foil (1.5 mm $\times$ 5 mm) embedded in the surface of the glass on opposite sides of the vessel (cf. Fig. 1).

Electron microscopic examination of the film was performed using a Siemens Elmiskop 1 operating at 80 or 100 kv. In order to correlate microscopic observations with area and resistance measurements, the films from which microscope specimens were to be obtained were prepared under the same conditions and specimens were obtained by smashing the glass vessel. For examination in transmission the film was stripped from the glass substrate by resting it in

* The authors are grateful to Mr. I. Nish of the Defence Standards Laboratory, Melbourne for supplying the chromium wire and analytical data for it.

the surface of a 10% solution of hydrofluoric acid until peeling at the edge just commenced, then rapidly transferring the sample to distilled water from the surface of which metal specimens were recovered on standard 200 mesh grids. Replication by shadowing with carbon/platinum (20° incident angle) was used with some nickel specimens, the replicas being recovered by solution of the nickel in hydrochloric acid.

No variation in film structure was apparent in fields selected from different parts of a grid, so that even at high magnifications fields shown are representative. The average crystal width for a field was calculated from counts of intercepts with random lines using Smith's (*10*) relation

$$\bar{N}/\bar{L} = 2/\pi(l/A)$$

where a random line of length $\bar{L}$ makes $\bar{N}$ intercept with crystal boundaries and l is the total boundary length in a total area A: The average crystal width was then taken to be given by $4A/l$, valid for circular crystals.

Influence of Condensation Rate on Surface Area

The rate of condensation, expressed as the average rate of arrival of atoms per unit geometric film area, was varied in two independent ways—by alteration of the total geometric condensing area using vessels of different diameter, and by altering the evaporation rate. There is good evidence that for nickel films produced under standardized conditions, surface area is proportional to film weight [Beeck *et al.* (*1*)], and this relation has been used to normalize measured areas to the basis of a 10 mg film weight. In Fig. 2 is shown the dependence of surface area per 10 mg on the rate of film condensation for nickel and tungsten deposited on to the substrate at 273°K.

It is apparent that the rate of condensation has a marked influence on the surface area of the films: low rate of condensation results in films of high specific area. Failure to control the rate of condensation or allow for its effect could be the major source of

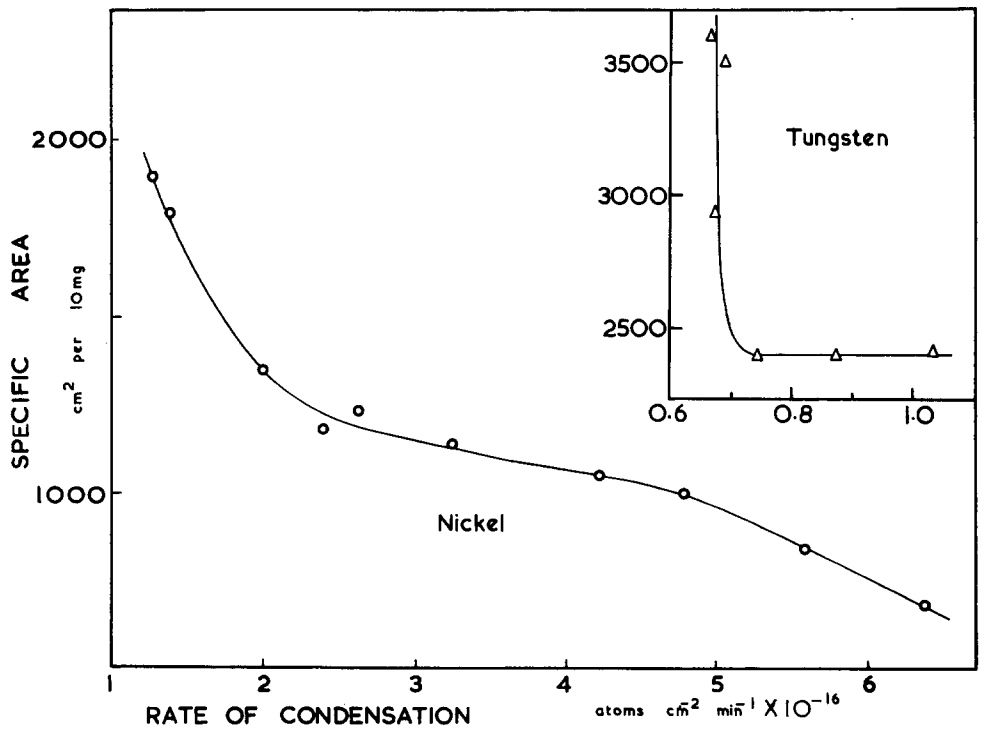

FIG. 2. The effect of condensation rate on film area.

irreproducibility encountered in adsorption and catalysis on films. This factor has not been recognized by others, with the exception of Singleton (*11*) who noted that a constant evaporation rate was necessary to achieve reproducible results on nickel films.

The power dissipation by the evaporation filament was about 180 watts and 30 watts for tungsten and nickel, respectively. Taking the thermal conductivity of Pyrex glass as 0.002 cal $cm^{-1}sec^{-1}(°C)^{-1}$, the glass wall thickness 1 mm and the area of the wall of the vessel 180 cm^2, the calculated temperature difference across the glass wall of the vessel is about 12°C for tungsten and 2°C for nickel. The maximum variation in power dissipation required to accommodate the range of evaporation rates for nickel and tungsten is about 6% and it is thus clear that the dependence of film area on evaporation rate cannot arise from a change in the temperature of the substrate.

In the subsequent sintering studies the rates of condensation of nickel films were within the range $2\text{–}4 \times 10^{16}$ atoms cm^{-2}-min^{-1}, and for tungsten films, in the range $0.8\text{–}1.0 \times 10^{16}$ atoms $cm^{-2}min^{-1}$.

Nickel Films Deposited at 273°K

Nickel films deposited at 273°K consisted of crystals with widths in the range 200–1000Å (Fig. 3), although in a specimen from near the edge of the film where it was thin, the average crystal width was 260Å. The replica of the surface (Fig. 4) shows that the surface of the film consists of asperities of dimensions comparable to the crystals. An examination of the diffraction pattern from the specimen normal to the electron beam and also tilted about 45° to the beam failed to reveal any preferred orientation of the crystals.

Thin white areas up to 20Å wide between the crystals are clearly visible at high magnifications (Fig. 5). Their appearance, and the behavior of their contrast in pictures slightly out of focus show that these are gaps between the crystals. Further confirmation of this interpretation was obtained by examining a curved specimen, when the gaps lying parallel to the axis of tilt were observed to disappear as the angle of tilt increased. The failure to observe gaps in nickel films after thermal treatment (see later) is taken to be evidence

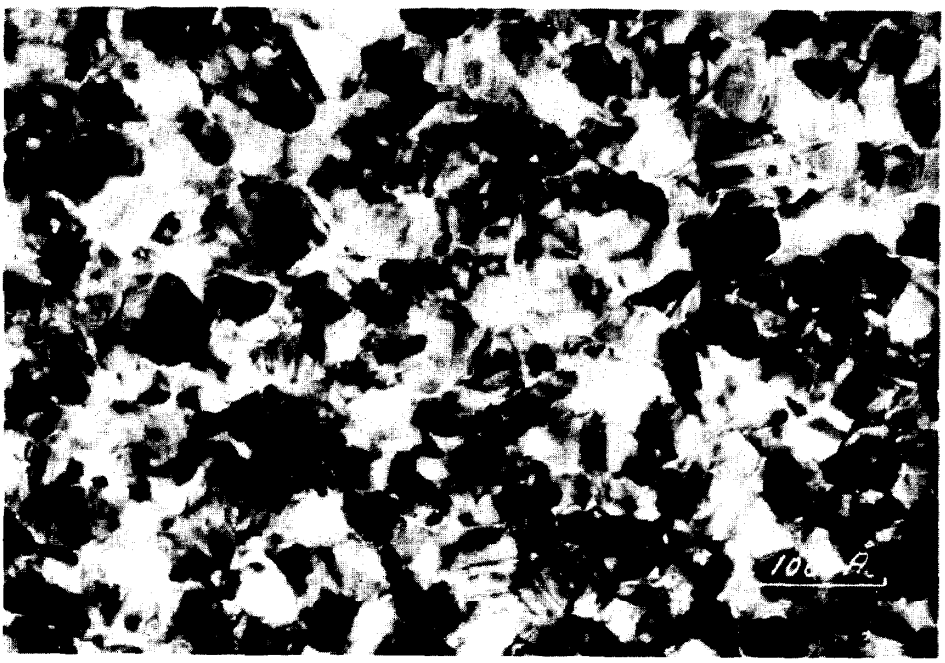

Fig. 3. Nickel, transmission.

FIG. 4. Nickel, replica.

FIG. 5. Nickel, high primary magnification, showing details of gaps.

that the gaps observed in unheated films did not originate during the stripping process.

All the crystals in the image contain some detailed contrast. Because they are small, contain no dislocations, and touch other crystals at only a few points, it is considered that this contrast arises mainly

from the shape of the crystals rather than from elastic strains within them. In many cases, where crystals are oriented to give suitable diffraction conditions, sets of fringes can be distinguished within the individual crystals (Fig. 6). These are interpreted as being extinction fringes, their number being a measure of the change of thickness, and their shape and spacing giving information about the shape of the crystal because any selected fringe is a contour line of constant thickness.

In Fig. 6, where they can be distinguished, four extinction contours can generally be counted. Unfortunately in the bright field pictures there is no detailed knowledge about the diffraction conditions of any selected crystal, but it seems likely that when the fringes are prominent, either a (*111*) or (*200*) reflection is operating. From the known extinction distances for nickel—258Å for (*111*) and 302Å for (*200*) (*12*)—four extinction contours indicate that the thickness of these crystals changes by 750–1000Å from the center to the edge. Most of this change occurs in the outer part of the crystal so that there is a central irregular plateau. The many irregularities in these fringes show that the crystal surfaces are correspondingly rough. The fields show only a comparatively few overlapping crystal boundaries so it is concluded that, in general, this nickel film is only one crystal in depth. This conclusion is also supported by a comparison of the crystal depth estimated from the extinction contours with the film thickness expected from the film weight and geometric area.

Although these nickel crystals appear to touch at points, they do not in general meet along boundaries. Since a large number of gaps $\leqslant$20Å can be seen in a field of random crystals each of depth $\sim$1000Å, it is improbable that the minimum gap width extends over an appreciable depth of crystal; thus the crystal thickness measured normally to the average film surface decreases at the crystal boundary to a thickness probably of a magnitude comparable to the gap width.

FIG. 6. Nickel, enlargement of Fig. 3, showing details of extinction contours.

It was found that varying the condensation rate for nickel in the range 3×10^{16}–2.7×10^{15} atoms $cm^{-2}min^{-1}$ resulted in no significant changes in the average crystal width. The effect of thermal radiation from the evaporation filament in influencing the

crystal width was examined by depositing a film in the presence of an auxiliary nickel filament (0.5 mm diameter) which was heated (4.0 amp) to just below the evaporation temperature and which was positioned to be, at the nearest, about 10 mm from the film. Examination of specimens taken from those regions of the film nearest to the auxiliary filament showed an increase by a factor of about 2 in average crystal width. It thus seems likely that since the thin parts of the film are the furthest from the filament, the lower thermal radiation in these regions contributes to the smaller average crystal width.

A faint extra ring in the nickel diffraction pattern was observed between the (*200*) and (*220*) rings and attributed to the presence of a small amount of nickel oxide. The nickel oxide pattern was easily distinguished in a field from which metallic nickel had been removed by dilute hydrochloric acid. From the ring width the oxide crystals were estimated to be ~50Å in size while from the relative intensities of the nickel and nickel oxide rings the oxide layer was estimated to be 50–100Å thick. The specimen from which metallic nickel had been partly removed was shadowed with Au/Pd and electron microscopic examination showed that the crystals of metallic nickel lay on top of the oxide layer in the sense that the film as originally deposited consisted of glass/oxide/nickel. The oxide layer itself showed little evidence of structure. The oxide almost certainly forms in the early stages of film deposition from residual oxygen in the vacuum system and possibly from oxide in the filament itself. It is apparent that the film grows on an oxide substrate, not glass. It was shown by Anderson and Baker (*7*) that the surface areas of nickel films measured by xenon adsorption were equal to the areas obtained by hydrogen adsorption: This agreement was achieved despite the presence of an oxide layer because the chemisorption of hydrogen on nickel oxide amounts to $<1\%$ of a monolayer even at 273°K [Cotton and Fensham (*13*)] while the adsorption of xenon on nickel oxide would be expected to occur at much higher pressures than on nickel [cf. Shereshefsky and Mazumder (*14*)].

Thermal Treatment of Nickel Films

It has been shown (*7*) that the surface area of a nickel film deposited at 273°K is reduced by heating to 468°K and that the rate of sintering, but not the ultimate extent, is reduced by the presence of chemisorbed hydrogen. Further data for sintering in 15 mm Hg pressure of hydrogen at 420°K was obtained by measuring the surface area at intervals on a single film. This data is compared with that at 468°K [Fig. 7 of ref. (*7*)] in a plot of log $(A - A_\infty)$ versus time (Fig. 7), where A is the area

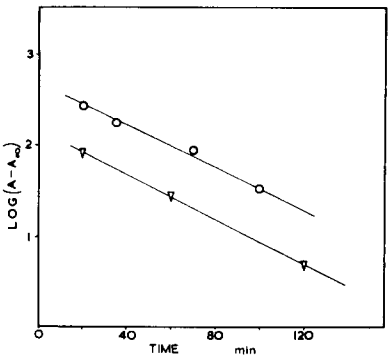

Fig. 7. Sintering of nickel films in hydrogen, ○ at 463°K, ▽ at 420°K.

at time t and A_∞ the ultimate area, taken as 605 cm² at 468°K and 630 cm² at 420°K. The linear relation found at times >20 min indicates first order dependence on $(A - A_\infty)$ but the initial sintering occurs by a much faster process.

For the slower process at times >20 min the activation energy is not greater than 5 kcal mole^{-1}, which is in agreement with the results of Roberts (*15*) who found that for iron films the activation energy for sintering was about 4 kcal mole^{-1}.

The changes in structure accompanying sintering of the films are shown in the electron micrographs, and Table 1 summarizes the measurements of grain width and surface area. Heating a nickel film in vacuum at 500°K for about 2 min (Fig. 8) resulted in no change in width for most crystals, although Fig. 8 shows that at isolated

TABLE 1

NICKEL AND TUNGSTEN FILMS SUBJECTED TO THERMAL TREATMENT

Temperature of deposition (°K)	Film weight (mg)	Thermal treatment after deposition	Average crystal width after treatment (Å)	Film area before thermal treatment (cm^2)	Film Area after thermal treatment (cm^2)	Fig. no.
		Nickel				
273	11.6	—	460	1430	—	3
273	14.2	500°K, ~2 min, vacuum	460[a]	1590	440	8
273	5.1	670°K, 60 min, vacuum	2000–3000	—	400[b]	11
273	9.3	470°K, ~5 min, hydrogen	460	—	—	9
273	7.6	470°K, 75 min, hydrogen	1000–1500	1300	600[b]	—
273	11.4	670°K, 60 min, hydrogen	2000–3000	—	—	—
273	8.8	420°K, 120 min, hydrogen	—	1120	635[b]	—
		530°K, further 60 min, hydrogen	—	635	430[b]	—
470	6.4	—	—	230	—	—
		Tungsten				
273	12.0	—	70	3250	—	14
273	10.4	670°K, 40 min, vacuum	80	—	2880	—
670	12.4	—	110	1130	—	13

[a] A few large crystals—see text.

[b] From the known behavior of films (7) these figures represent the ultimate areas reached at these temperatures.

points in the film, crystal growth had occurred leading to the production of a few large crystals up to about ten times the average crystal dimension. However, no gaps between the crystals can be detected for this specimen, nor was it possible to observe any changes of contrast at the crystal boundaries when focussing conditions were slightly altered.

From Fig. 9 it is seen that heating a

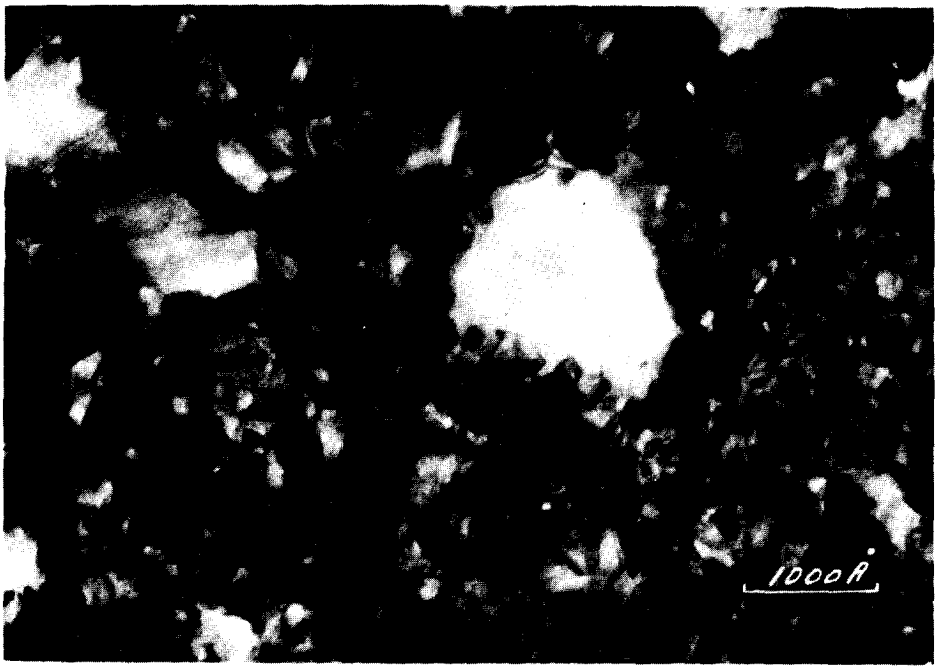

FIG. 8. Nickel, heated to 500°K in vacuum for 2 min.

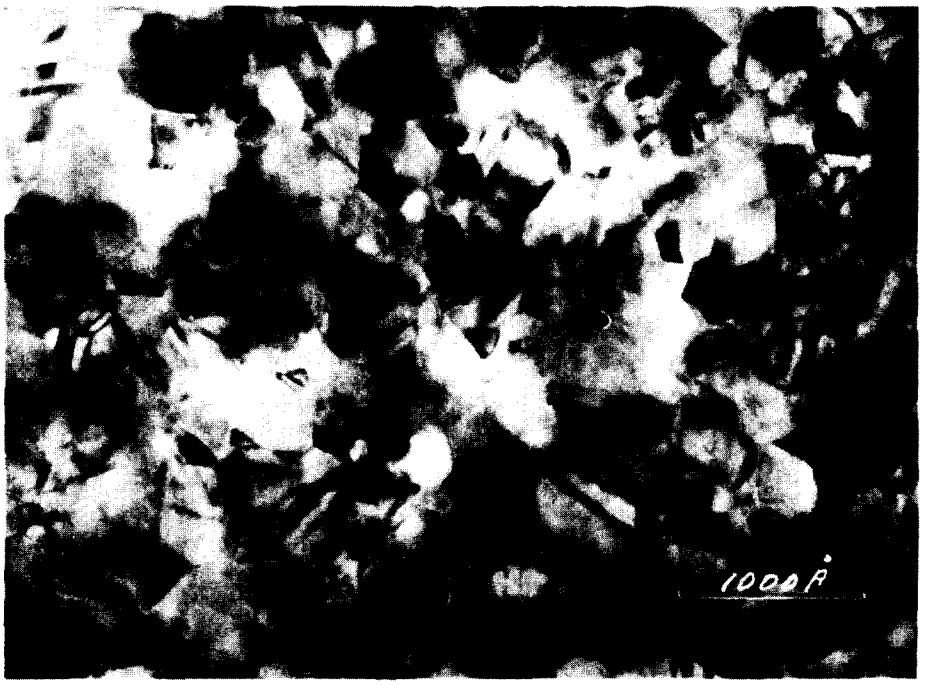

FIG. 9. Nickel, heated to 500°K in hydrogen for 5 min.

nickel film at 470°K for about 5 min in 15 mm Hg pressure of hydrogen resulted in the removal of gaps between the crystals but no change in the crystal size. Where extinction contours are resolved they are now usually sharper and fewer in number, indicating that the difference in thickness between the center and the edge of the

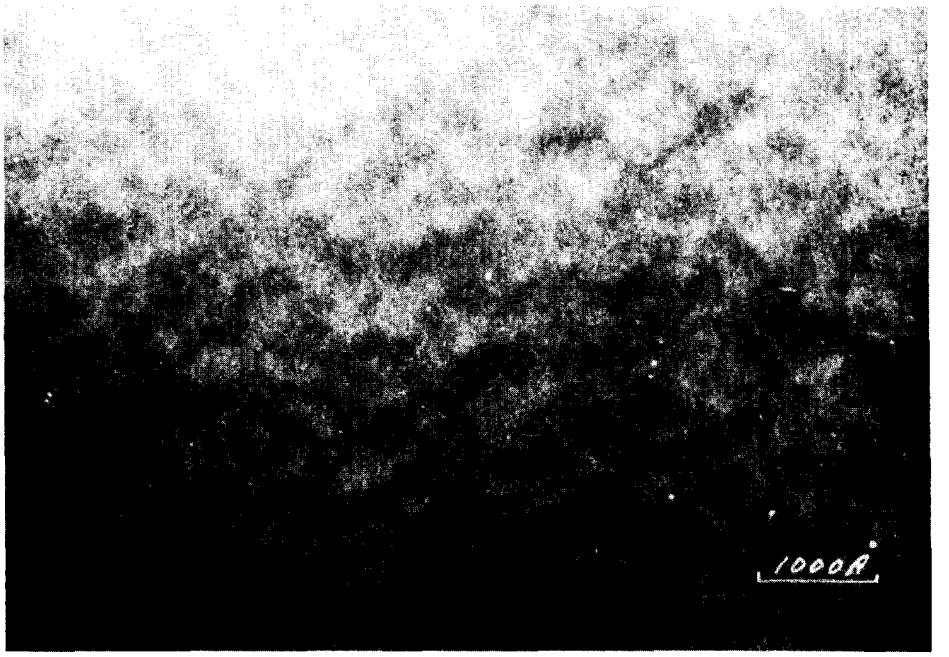

FIG. 10. Nickel, as Fig. 9, replica.

FIG. 11. Nickel, heated to 670°K in vacuum for 60 min.

crystals is less than that in the unheated specimens and that the surfaces are smoother. A replica of the same specimen (Fig. 10) shows that a degree of surface roughness is still apparent, but the asperities are less well defined than in unheated films, in agreement with the above conclusion based on extinction contours. The

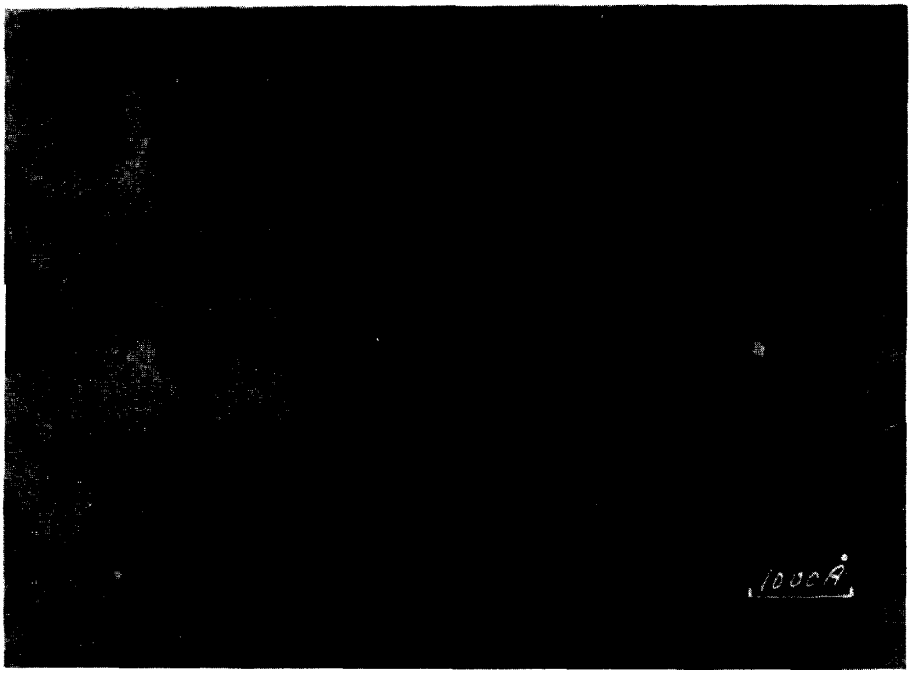

FIG. 12. Nickel, as Fig. 11, replica.

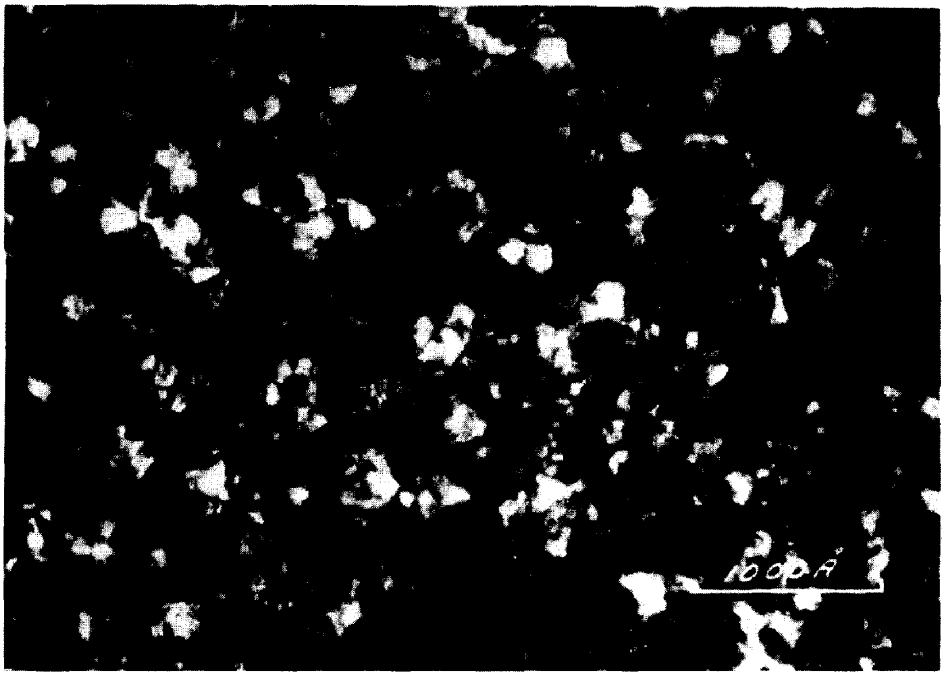

FIG. 13. Tungsten, condensed on substrate at 670°K.

FIG. 14. Tungsten, condensed on substrate at 273°K.

crystals apparently now meet at boundaries which are several hundred Å thick. Furthermore, there are fewer irregularities in the extinction contours, again showing that the crystal faces are smoother than those in the unheated specimens.

Figure 11 shows that heating a nickel film in vacuum at 670°K for 60 min re-

sulted in extensive crystal growth and a replica of the film surface after this treatment (Fig. 12) shows the elimination of the surface asperities and the production of a comparatively featureless surface. Similar results were obtained for nickel films similarly heated in 15 mm Hg pressure of hydrogen. The crystals, 2000–3000Å in width, no longer taper and the boundaries penetrate randomly through the film as in a bulk polycrystal. The faces of the crystals are much flatter, although some undulations can be detected in the outermost of the fringes from stacking faults and on the extinction contours.

Tungsten Films

The crystal width in films of tungsten is much less than that in nickel films, and the individual grains can be distinguished only in thin films and then less readily. The deposition of a tungsten film (cf. Table 1) on a substrate heated to 670°K (Fig. 13) resulted in an increase in crystal size by a factor ~1.5 and a reduction in surface area by a factor ~3, compared to a film deposited at 273°K (Fig. 14). However, a tungsten film deposited at 273°K and subsequently heated in vacuum at 670°K for 40 min showed little increase in crystal size or change in surface area.

Electrical Resistance Measurements

The resistance changes during the deposition of nickel and tungsten films at 273°K are shown in Fig. 15. For nickel, the resistance values for film weights 1.0, 3.8, 4.4, and 7.6 mg. were determined at the end of deposition and so the film weights have been directly measured. The remaining points for nickel and tungsten have been calculated from the time and final film weight assuming a constant rate of deposition.

To find the resistivity of films for comparison with the bulk metals, a gold film of known weight was deposited in the same vessel. Gold films sintered to 700°K have been shown by Scott (*16*) to have the resistivity of bulk gold. The measured resistance of a sintered gold film of weight 45 mg was 1.75 ohm at 273°K and these data have been used, together with the estimated thicknesses to provide a scaling factor for the calculation of resistivities from film resistances of nickel and tungsten. The thickness of the gold film was estimated at about 2000Å and thus each of the two current paths of 70 mm length through the film between the platinum con-

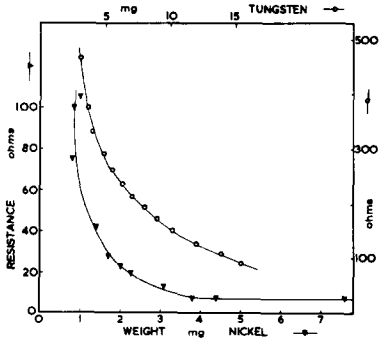

Fig. 15. Electrical resistance of nickel and tungsten films.

tacts (Fig. 1) are estimated to have an effective width of 2.4 mm. The calculated resistance of a nickel film of 5 mg weight having the resistivity of bulk nickel is ~4 ohm which is about half the resistance observed for films of normal weight deposited at 273°K, but about equal to the ultimate resistance after sintering (cf. Table 2). Similarly the resistivity of a tungsten film deposited at 273°K is approximately 20 times that of bulk tungsten but falls to a value about 3 times greater after sintering at 600°K.

The magnitude of the contact resistance R_c between individual nickel crystals may be obtained in terms of the measured film resistance if the conduction path through the film is considered as a two-dimensional resistance net. If this net is approximated by a square array of resistances, each R_c, it is easily shown that the total film resistance is given by $N_l R_c / N_w$, where N_l is the total number of resistances in one lengthwise chain and N_w is the number of these chains across the width of the net. For nickel crystals of average width 460Å and with each of the two current paths through the film having effective dimensions 70 mm $\times$ 2.4 mm (see above), values of

TABLE 2
RESISTANCE CHANGES FROM THERMAL TREATMENT OF NICKEL AND TUNGSTEN FILMS

Metal	Film wt (mg)	Thermal treatment	R_1, initial film resistance at 273°K (ohm)	R_2, film resistance at 273°K after thermal treatment (ohm)	$\frac{(R_1 - R_2)100}{R_2}$	Temperature coefficient of resistance (ohm deg^{-1})
Nickel	3.8	670°K, 60 min, vacuum	7.4	5.6	32	0.0035
Nickel	4.7	460°K, 40 min, vacuum	7.5	4.1	83	0.0033
Nickel	7.6	470°K, 75 min, vacuum	7.9	3.2	147	0.0035
Nickel	4.4	450°K, 126 min, hydrogen	7.5	4.7	60	0.0035
		then, 530°K, 120 min, hydrogen	4.7	4.1	15	0.004
Tungsten	15.8	290°K, 120 min, vacuum	89	52	71	—
		then, 490°K, 12 min, vacuum	52	30.5	70	0
		then, 600°K, 50 min, vacuum	30.5	30.5	0	0

1.52×10^6 and 0.52×10^5 are estimated for N_1 and N_w, respectively, and thus the observed film resistances of ~8 ohm require $R_c \simeq 0.3$ ohm. Holm (*17*) has shown that for normal metallic conduction across a contact

$$R_c \simeq 10^8 \rho / 2d$$

where d(Å) is the contact diameter and ρ the resistivity. On this basis, for $R_c \simeq 0.3$ ohm, $d \simeq 1300$Å. Despite the approximations involved in the calculation, this value of d is absurdly large and we suggest that the failure of the above equation provides evidence for the contribution made by electron tunnelling between crystals where the gap width is sufficiently small, say <5Å. Both Broeder *et al.* (*18*) and, more recently Ehrlich (*19*) have speculated on the importance of electron tunnelling in film conductance and Milner and Tatarinova (*4*) have also concluded from a study of the electrical resistance and magnetic properties that nickel films consist of imperfectly touching crystals. We believe that the experimental establishment of the gap structure for unsintered nickel films presented in this paper makes it highly probable that in these films electron tunnelling makes a substantial contribution to the conductance. However, in sintered nickel films where gaps no longer exist, the tunnelling mechanism is presumably absent and this is in agreement with the values for the temperature coefficient of resistance (Table 2) which are comparable with bulk nickel. On the other hand, it has been shown [Anderson and Baker (*7*) and cf. Table 1] that tungsten films deposited at 273°K are highly resistant to sintering and thus the thermally treated tungsten films to which reference is made in Table 2 presumably have retained a gap structure resulting in an electron tunnelling contribution to the conductance and this is in agreement with the observed zero value for the temperature coefficient of resistance.

A calculation of contact resistance in tungsten films similar to that provided above for nickel is not warranted because of the possibility (see next section) that tungsten films are many crystals thick.

COMPARISON OF VARIOUS METALS

Transmission electron diffraction patterns showed all films to have the same crystal structure as the bulk metal and, in particular tungsten films had the usual body-centered cubic structure rather than the A 15 structure found for some tungsten films by Moss and Woodward (*20*).

The study of other metals deposited at 273°K was confined to measurements of the surface area by xenon adsorption, and crystal widths from electron micrographs of the films subsequently stripped from the glass. For tungsten, molybdenum, and rhodium, where the crystals are very small, the averages were obtained by random measurements of individual crystals; for the rest the intercept method was used. The widths may be underestimated slightly, particularly for the finest grained films, because it was necessary to use parts of the

film away from the central area to obtain micrographs sufficiently clear to enable crystals to be resolved. The percentages of surface atoms are calculated from the measured surface areas and in general are comparable with the results of Brennan, Hayward, and Trapnell (*21*). Precise agreement is not expected because of differing conditions of film deposition. In the case of palladium, however, Brennan, Hayward, and Trapnell found 0.9% surface atoms for a 37 mg film and it appears reasonable to conclude that, at least for this metal, the area is not proportional to the film weight. This lack of proportionality may be associated with the structure of gaps in the film which regulate the accessibility of the interior of the film to the gas.

The data of Table 3 show that there is a general trend for the percentage of surface atoms to decrease as the crystal width increases. We have shown that for nickel films the crystals penetrate from top to bottom. Because of the smaller crystal widths similar evidence for the other metals is lacking. However, for comparison with the measured film areas, the last column of Table 3 contains areas computed on the assumption that all the films are one crystal thick and that the individual crystals are regular circular prisms. On this model the width of the crystals is thus determined primarily by the nucleation process in the initial layers and subsequent deposition merely propagates this structure. Nevertheless, it is clear that a detailed discussion of the mechanism of film growth cannot be attempted until unequivocal evidence is available about the height of individual crystals in relation to the total film thickness, that is whether during film growth the process of successive nucleation of metal crystals on the surface of growing crystals is important.

TABLE 3
METAL FILMS DEPOSITED AT 273°K

Metal	Average rate of condensation (atom cm^{-2} min^{-1} $\times 10^{-16}$)	Film weight (mg)	Area (cm^2)	Per cent surface atoms	Average crystal width (Å)	Calculated area (cm^2)
Tungsten	0.9	12.0	3250	11.2	70	3830
Molybdenum	0.95	3.8	2580	14.7	75	2410
Rhodium	0.9	6.1	2020	7.5	80	2610
Chromium	4.6	5.4	2600	6.8	130	2710
Palladium	0.4	4.0	620	3.5	160	970
Platinum	0.3	6.2	840	5.5	180	790
Iron	7.1	6.6	1970	4.5	240	1580
Nickel	3.2	11.6	1430	1.9	460	1270

THE PROCESS OF FILM SINTERING

It was established previously (*7*) from area measurement that the presence of hydrogen markedly reduces the rate of sintering of nickel films. The present results have confirmed this but failed to reveal any further effect of hydrogen.

Two distinct phases can be distinguished during the heating of nickel films. Whether in hydrogen or in vacuum the initial process is the closure of the gaps between the crystals and since this is relatively rapid and would be expected to shut off the lower surfaces of the crystals from access by gas, it is apparently responsible for the initial rapid fall in surface area. Asperities are still present on the surface of the film after gap closure and these are removed during the next stage of sintering. If the surface asperities are treated as close-packed hemispheres, their removal would result in a reduction of surface area by a factor of $\sim$1.8. This model probably overestimates the height of the asperities and no doubt the elimination of some steps and terraces on the crystal faces also contributes to the area reduction. It was shown (cf. Table 1) that the film area can approach the ultimate value before any extensive crystal

growth occurs: In this sense crystal growth has but little effect on film area.

The data in Table 1 show that both for nickel and tungsten the area resulting from film deposition at an elevated temperature is considerably below the area for a film which had been sintered at that temperature subsequent to deposition at 273°K, and furthermore, the former results in the formation of abnormally large crystals. We believe that this is due to the increased ease of surface migration of the condensing atoms at the elevated temperature and the effect is in agreement with the prediction of Shockley (*22*).

REFERENCES

1. BEECK, O., SMITH, A. E., AND WHEELER, A., *Proc. Roy. Soc.* (*London*) **A177**, 62 (1940).
2. PICARD, R. G., AND DUFFENDACK, O. S., *J. Appl. Phys.* **14**, 291 (1943).
3. LEVINSTEIN, H., *J. Appl. Phys.* **20**, 306 (1949).
4. MIL'NER, A. S., AND TATARINOVA, L. I., *Fiz. metal. i. metalloved. Akad. Nauk. SSSR., Uval Filial* **9**, 673 (1960).
5. SACHTLER, W. M. H., DORGELO, G. J. H., AND VAN DER KNAAP, W., *J. chim. phys.* **51**, 491 (1954).
6. GUNDRY, P. M., AND TOMPKINS, F. C., *in* "Chemisorption" (W. E. Garner, ed.), p. 152. Butterworths, London, 1956.
7. ANDERSON, J. R., AND BAKER, B. G., *J. Phys. Chem.* **66**, 482 (1962).
8. KEMBALL, C., *Proc. Roy. Soc.* (*London*) **A214**, 413 (1952).
9. ANDERSON, J. R., AND KEMBALL, C., *Proc. Roy. Soc.* (*London*) **A223**, 361 (1954).
10. SMITH, C. S., "Metal Interfaces," p. 102. Am. Soc. for Metals, Cleveland, Ohio, 1952.
11. SINGLETON, J. H., *J. Phys. Chem.* **60**, 1606 (1956).
12. HIRSCH, P. B., HOWIE, A., AND WHELAN, M. J., *Phil. Trans. Roy. Soc.* (*London*) **A252**, 499 (1960).
13. COTTON, J. D., AND FENSHAM, P. F., results to be published, this laboratory.
14. SHERESHEFSKY, J. L., AND MAZUMDER, B. R., *J. Phys. Chem.* **63**, 1630 (1959).
15. ROBERTS, M. W., *Trans. Faraday Soc.* **56**, 128 (1960).
16. SCOTT, H. G., private communication, 1960.
17. HOLM, R., "Electric Contacts Handbook," 3rd ed., p. 44. Springer-Verlag, Berlin, 1958.
18. BROEDER, J. J., VAN REYEN, L. L., SACHTLER, W. N. H., AND SCHUIT, G. C. A., *Z. Elektrochem.* **60**, 841, (1956).
19. EHRLICH, G., *J. Chem. Phys.* **35**, 2165 (1961).
20. MOSS, R. L., AND WOODWARD, I., *Acta Cryst.* **12**, 255 (1959).
21. BRENNAN, D., HAYWARD, D. O., AND TRAPNELL, B. M. W., *Proc. Roy. Soc.* (*London*) **A256**, 81 (1960).
22. SHOCKLEY, W., *in* "Structure and Properties of Thin Films" (Neugebauer, C. A., Newkirk, J. B., and Vermilyea, D. A., eds.), p. 537. Wiley, New York, 1959.